CHEST

A predictive model and scoring system combining clinical and CT characteristics for the diagnosis of COVID-19

Le Qin[1] · Yanzhao Yang[1] · Qiqi Cao[1] · Zenghui Cheng[1] · Xiaoyang Wang[2] · Qingfeng Sun[3] · Fuhua Yan[1] · Jieming Qu[4] · Wenjie Yang[1]

Abstract

Objectives To develop a predictive model and scoring system to enhance the diagnostic efficiency for coronavirus disease 2019 (COVID-19).

Methods From January 19 to February 6, 2020, 88 confirmed COVID-19 patients presenting with pneumonia and 80 non-COVID-19 patients suffering from pneumonia of other origins were retrospectively enrolled. Clinical data and laboratory results were collected. CT features and scores were evaluated at the segmental level according to the lesions' position, attenuation, and form. Scores were calculated based on the size of the pneumonia lesion, which graded at the range of 1 to 4. Air bronchogram, tree-in-bud sign, crazy-paving pattern, subpleural curvilinear line, bronchiectasis, air space, pleural effusion, and mediastinal and/or hilar lymphadenopathy were also evaluated.

Results Multivariate logistic regression analysis showed that history of exposure ($\beta = 3.095$, odds ratio (OR) = 22.088), leukocyte count ($\beta = -1.495$, OR = 0.224), number of segments with peripheral lesions ($\beta = 1.604$, OR = 1.604), and crazy-paving pattern ($\beta = 2.836$, OR = 2.836) were used for establishing the predictive model to identify COVID-19-positive patients ($p < 0.05$). In this model, values of area under curve (AUC) in the training and testing groups were 0.910 and 0.914, respectively ($p < 0.001$). A predicted score for COVID-19 (PSC-19) was calculated based on the predictive model by the following formula: PSC-19 = 2 × history of exposure (0–1 point) − 1 × leukocyte count (0–2 points) + 1 × peripheral lesions (0–1 point) + 2 × crazy-paving pattern (0–1 point), with an optimal cutoff point of 1 (sensitivity, 88.5%; specificity, 91.7%).

Conclusions Our predictive model and PSC-19 can be applied for identification of COVID-19-positive cases, assisting physicians and radiologists until receiving the results of reverse transcription–polymerase chain reaction (RT-PCR) tests.

Key Points

• *Prediction of RT-PCR positivity is crucial for fast diagnosis of patients suspected of having coronavirus disease 2019 (COVID-19).*
• *Typical CT manifestations are advantageous for diagnosing COVID-19 and differentiation of COVID-19 from other types of pneumonia.*
• *A predictive model and scoring system combining both clinical and CT features were herein developed to enable high diagnostic efficiency for COVID-19.*

Keywords Tomography, x-ray computed · COVID-19 · Pneumoni · Predictive value of tests

---

Le Qin and Yanzhao Yang contributed equally to this work.

Wenjie Yang and Jieming Qu are co-corresponding authors.

✉ Jieming Qu
  jmqu0906@163.com

✉ Wenjie Yang
  lisa_ywj@163.com

[1] Department of Radiology, Shanghai Jiao Tong University Medical School Affiliated Ruijin Hospital, No. 197, Ruijin Er Road, Shanghai 200025, China

[2] Department of Radiology, Ruian People's Hospital, No. 108, Wan Song Road, Ruian 325200, Zhejiang Province, China

[3] Department of Infectious Diseases, Ruian People's Hospital, No. 108, Wan Song Road, Ruian 325200, Zhejiang Province, China

[4] Department of Respiratory and Critical Care Medicine, Shanghai Jiao Tong University Medical School Affiliated Ruijin Hospital, NO. 197 Ruijin Er Road, Shanghai 200025, China

⦿ Springer

Abbreviations

AUC	Area under curve
CAP	Community-acquired pneumonia
CDC	Centers for Disease Control and Prevention
CI	Confidence interval
COVID-19	Coronavirus disease 2019
CRP	C-reactive protein
GGO	Ground glass opacity
OR	Odds ratio
PSC-19	Predictive score for COVID-19
ROC	Receiver operating characteristic
RT-PCR	Reverse transcription–polymerase chain reaction
SARS-CoV-2	Severe acute respiratory syndrome coronavirus 2
WHO	World Health Organization

Introduction

In December 2019, an outbreak of severe acute respiratory syndrome coronavirus 2 (SARS-CoV-2) infection was reported in Wuhan, Hubei Province, China [1]. On February 12, 2020, the World Health Organization (WHO) officially named the disease as coronavirus disease 2019 (COVID-19). The human-to-human transmission of COVID-19 can be realized through respiratory droplets, direct contact, and even a fecal–oral route [2, 3]. Although prevention and control measures have been applied, COVID-19 cases are no longer limited in Wuhan. Concerning the continuously increased number of infected patients and countries, the WHO adjusted the risk of spread of COVID-19 to "very high at a global level" on February 28, 2020. Therefore, rapid diagnosis of infected patients is indeed vital.

The common clinical symptoms of COVID-19 include fever, cough, headache, or fatigue. Patients can present normal or abnormal leukocyte counts, lymphopenia, or thrombocytopenia, with extended activated thromboplastin time and increased C-reactive protein (CRP) level [1–3]. The comorbidities including respiratory failure, acute respiratory distress syndrome, acute renal injury, and acute cardiac injury can also occur in severe cases, resulting in the poor prognosis of patients. Radiological examinations are highly significant for the early detection and management of COVID-19. To date, the reported typical chest CT manifestations involve multifocal bilateral patchy ground glass opacity (GGO) and consolidation, with a peripheral, posterior and lower predominance in the lungs [4, 5].

At present, reverse transcription–polymerase chain reaction (RT-PCR) test remains the reference standard to make a definitive diagnosis of COVID-19 infection. The COVID-19 RT-PCR test aims to qualitatively detect nucleic acid from SARS-CoV-2 in upper and lower respiratory specimens

(e.g., nasopharyngeal or oropharyngeal swabs, sputum, lower respiratory tract aspirates, bronchoalveolar lavage, and nasopharyngeal wash/aspirate or nasal aspirate) collected from individuals suspected of having COVID-19. However, several studies demonstrated that COVID-19 patients with pulmonary involvement on CT could have negative results of RT-PCR, including 36 of 51 (71%) patients reported by Fang et al [6], 5 of 167 (3%) patients presented by Xie et al [7], and a case introduced by Huang et al [8]. RT-PCR tests were repeated for these patients and positive results achieved thereafter. The reasons for false-negative RT-PCR results may be related to limitation of nucleic acid detection technologies, inappropriate methods of sampling, low viral load in patients, or improper timing of sampling for RT-PCR. Furthermore, RT-PCR test is generally performed by the Centers for Disease Control and Prevention (CDC), and it cannot be therefore carried out on-site. This workflow may be time-consuming and cause delay in the final diagnosis.

The fever observation department, as an independent emergency department dedicated to patients with fever, was rapidly established in China. It undertakes diagnosis and investigation of suspected patients, as well as being the frontline of screening and diagnosing patients with COVID-19. Differential diagnosis is crucial to the early quarantine of suspected patients with fever and the prevention of transmission. Non-SARS-CoV-2 infected pneumonia, basically community-acquired pneumonia (CAP), which has similar clinical symptoms and imaging findings, mimicking COVID-19 pneumonia, remains the most frequent lung disease to be differentiated in the fever observation department.

Therefore, the purpose of the present study was to develop a predictive model and scoring system to improve the diagnostic efficiency for COVID-19 via analysis of clinical features, laboratory data, and CT manifestations of study subjects presenting with COVID-19 pneumonia versus non-COVID-19 pneumonia.

Materials and methods

Study subjects and design

This retrospective bi-center study was approved by the Institutional Review Board. Written informed consent was waived. Herein, from January 19 to February 6, 2020, 311 patients were enrolled at the fever observation department. Inclusion criteria for patients suspected of COVID-19 were set according to the sixth edition of the Diagnosis and Treatment Program of COVID-19 proposed by The National Health Commission of the People's Republic of China: (1) epidemiological history: history of travel to Wuhan or history of residence in Wuhan or other areas with continuous transmission of local cases within 14 days before the onset of the

disease, history of contact with COVID-19 patients within 14 days before the onset of the disease, and clustering or epidemiological association with COVID-19, and (2) clinical features: fever and/or disorder of the respiratory system, imaging manifestations of COVID-19 pneumonia, normal or reduced leukocyte count, or reduced lymphocyte count. Patients with epidemiological history and any two of the three above-mentioned clinical features and patients without epidemiological history and with all the three clinical features were classified by the multiple-disciplinary expert group as suspected [9].

All the suspected patients were tested by RT-PCR. Throat and nose swab specimens were obtained. A total of 106 patients with positive results of RT-PCR tests conducted at Shanghai Municipal CDC were included and considered as COVID-19-positive cases. The RT-PCR tests were repeated for 21 COVID-19 patients because results of the first RT-PCR tests were negative. Patients with negative chest CT manifestation ($n = 12$, 11.3%), missing data ($n = 5$, 4.7%), and poor quality of CT images ($n = 1$, 0.9%) were excluded. Cases with the negative results of RT-PCR tests at least twice consecutively were considered as non-COVID-19. For 205 with negative results of RT-PCR, pneumonia was diagnosed based on the Infectious Diseases Society of America/American Thoracic Society (IDSA/ATS) guidelines [10]. In brief, patients with at least one of the clinical symptoms of cough, sputum, fever, dyspnea, and pleuritic chest pain, plus at least one finding of coarse crackles on auscultation or elevated inflammatory biomarkers, in addition to a new pulmonary infiltration on chest CT, were diagnosed to have pneumonia. Patients with poor quality of medical images ($n = 6$, 2.9%), negative chest CT manifestation ($n = 78$, 38.0%), lung cancer

Table 1 Etiology of COVID-19-negative cases

Etiology	Number of patients
Bacterial infection	33
Mycobacterium tuberculosis complex	2
Influenza virus A	2
Influenza virus B	1
Influenza virus B and mycoplasma	2
Mycoplasma	1
Undetermined*	39
Total	80

*13 patients had negative respiratory tract IgM including legionella type 1; mycoplasma; *Coxiella burnetii*; *Chlamydia pneumoniae*; adnovirus; R syncytial virus A and B (RSVA and RSVB); influenza virus A and B (FluA and B); parainfluenza virus 1, 2, 3, and 4 (PIV1, 2, 3, and 4); coronavirus OC43 type; coronavirus 229E/NL63 type; human metapneumovirus (HMPV); human rhinovirus (HRV); enterovirus (EV); and human bocavirus (H BoV). And the other 26 patients had negative FluA and B IgM

($n = 3$, 1.5%), and missing data ($n = 38$, 18.5%) were excluded. Throat and nose swab specimens of COVID-19-negative patients were tested by IgM antibody and influenza viruses A and B as appropriate for the detection of etiology. Bacterial infection was also diagnosed according to the IDSA/ATS guidelines (Table 1) [10]. Finally, a total of 168 patients, including 88 COVID-19-positive and 80 COVID-19-negative subjects, were included in the present study (Fig. 1).

Clinical data

All the clinical data related to the subjects' demographic characteristics and laboratory results were retrospectively reviewed and collected.

Imaging data analysis

All images were downloaded from picture archiving and communication systems (PACS), and made anonymous by a computer engineer. Then, the images were uploaded to PACS for analysis. Two radiologists, each with more than 10 years of experience in thoracic imaging, who were blinded to clinical data reviewed all CT images in a consensus reading.

The location of the lesions was classified as the predominantly center and predominantly periphery according to the location at either the inner or outer half of the lung field. The attenuation of the lesions was classified as GGO, mixed GGO, and consolidation. In particular, a segment with mixed GGO was marked as both GGO and consolidation. Similarly, a segment with both peripheral and central lesions was symbolized with both periphery and center. The pattern of the lesions was sorted into patchy and oval. The oval lesion refers to a rounded or oval, well-circumscribed opacity, and the patchy lesion is an ill-defined and irregular opacity. The number of affected lung lobes and segments was also counted. Scores were achieved based on the size of the lesions as grade 1 (diameter, < 1 cm), grade 2 (diameter, 1–3 cm), grade 3 (diameter, 3 cm to 50% of the segment), or grade 4 (over 50% of the segment). Other CT features, such as air bronchogram, tree-in-bud sign, crazy-paving pattern, subpleural curvilinear line, bronchiectasis, air space, pleural effusion, and mediastinal and/or hilar lymphadenopathy were evaluated as well. All the terms were defined according to the glossary of terms for chest imaging presented by the Fleischner Society [11].
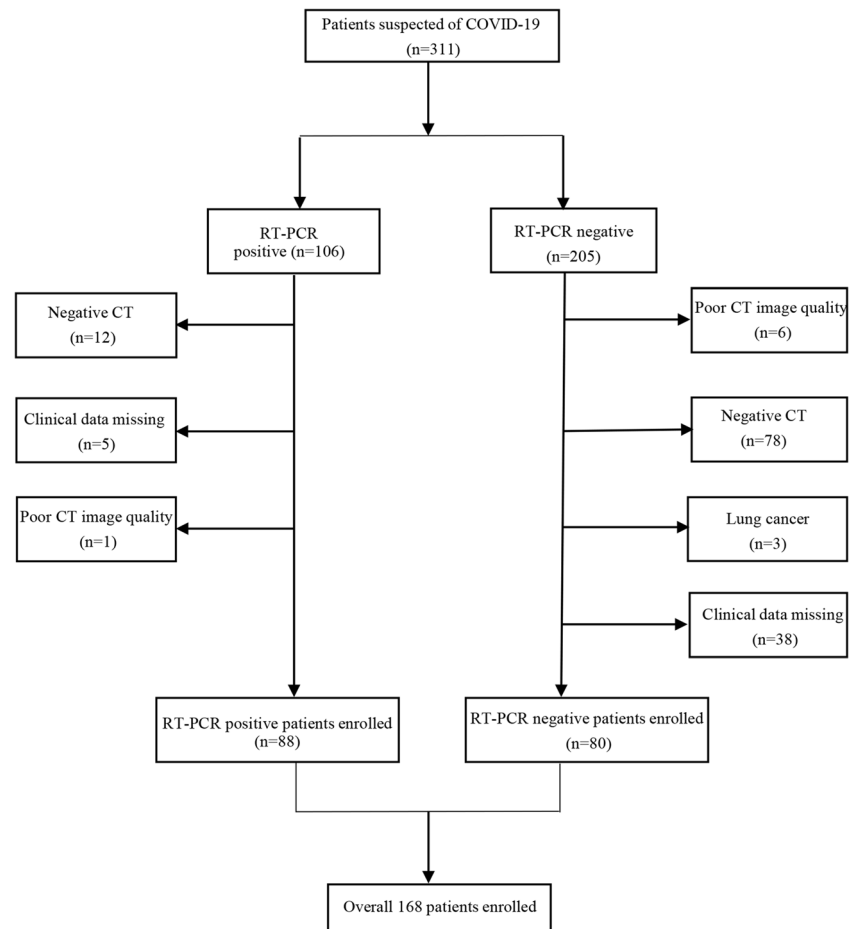
Statistical analysis

One hundred sixty-eight patients were randomly classified into a training group (118 patients, 70.2%, 62 COVID-19 and 56 non-COVID-19 patients) and a testing group (50 patients, 29.8%, 26 COVID-19 and 24 non-COVID-19 patients). Normally and abnormally distributed continuous data were expressed as mean ± standard deviation and median

Fig. 1 Flowchart of the study.
COVID-19, coronavirus disease
2019; RT-PCR, reverse
transcription–polymerase chain
reaction

(25th percentile, 75th percentile), respectively. These data were then analyzed by unpaired t test and Mann–Whitney U test, accordingly. The categorical data were expressed as count (%) and analyzed by chi-square test or Fisher's exact. Data with $p < 0.1$ were retained. Then, the continuous data were categorized. Due to the sample size of our training group, at most 10 variables were selected for multivariate logistic regression analysis. Logistic regression analysis was performed with stepwise forward likelihood ratio selection method. Cut-off values were identified by plotting the receiver operating characteristic (ROC) curve. Area under curve (AUC) was calculated for both training and testing groups. $p < 0.05$ was considered as statistically significant. All data were analyzed by SPSS 22.0 (IBM) and GraphPad Prism 8.0.2 (GraphPad Software Inc) software.

Results

Clinical data and CT features

Baseline characteristics of all 168 patients are summarized in Table 2. Data related to history of exposure, leukocyte count,

neutrophil count, platelet count, and time interval from symptom onset to CT scan were significantly different between COVID-19-positive and COVID-19-negative groups ($p < 0.001$). Regarding the CT features, the number of affected lobes and segments, segments with peripheral, GGO, consolidation, and patchy lesions in the positive group, was significantly higher than that in the negative group ($p < 0.001$). In addition, the air bronchogram, crazy-paving pattern, subpleural curvilinear line, and bronchiectasis were significantly more common in the positive group than in the negative group ($p < 0.05$). However, the tree-in-bud sign was significantly less common in the positive group compared with the negative group ($p < 0.001$). Table 3 presents CT manifestations.

Clinical and radiological risk factors for RT-PCR-positive

Clinical and laboratory results were categorized to 0–1 or 0–2 points for logistic regression analysis (Table 4). History of exposure [$\beta = 2.090$; odds ratio (OR) = 8.086; 95% CI (confidence interval), 3.339–19.583, $p < 0.001$] and leukocyte count ($\beta = -1.741$; OR = 0.175; 95% CI,

Table 2 Patients' clinical characteristics

Characteristics	COVID-19 ($n = 88$)	Non-COVID-19 ($n = 80$)	Overall ($n = 168$)	p value
Clinical characteristics				
Age	47.3 ± 12.4	42.8 ± 17.3	45.2 ± 15.1	0.053
Male	42, 47.7%	30, 37.5%	72, 42.9%	0.182
History of exposure	68, 77.3%	20, 25%	88, 52.4%	< 0.001
Laboratory tests				
Leukocyte count ($\times 10^9$ per L) (range, 3.5–9.5)	4.6 (3.5, 5.7)	6.8 (4.5, 9.1)	5.4 (3.9, 7.2)	< 0.001
Decrease	23	6	29	
Increase	1	17	18	
Neutrophil count ($\times 10^9$ per L) (range, 1.8–6.3)	2.9 (2.0, 3.9)	4.4 (2.7, 7.0)	3.3 (2.3, 5.2)	< 0.001
Decrease	17	7	24	
Increase	3	23	26	
Lymphocyte count ($\times 10^9$ per L) (range 1.1–3.2)	1.2 (1.0, 1.6)	1.3 (1.0, 1.9)	1.3 (1.0, 1.7)	0.115
Decrease	28	26	54	
Increase	2	2	4	
Platelet count ($\times 10^9$ per L) (range 125–350)	179.5 (141.0, 223.5)	217.5 (174.5, 274.8)	202 (152.3, 250.3)	< 0.001
Decrease	5	10	15	
Increase	5	4	9	
C-reactive protein (mg/L, 0.0–6.0)	8.6 (3.1, 23.4)	12.1 (3.1, 33.6)	10.1 (3.1, 25.5)	0.363
Increase	32	56	88	

COVID-19 coronavirus disease 2019

0.056–0.553, $p = 0.003$) were significantly associated with positive RT-PCR results for COVID-19 ($p < 0.001$). AUC values in the training and testing groups were 0.813 and 0.849, respectively ($p < 0.001$) (Fig. 2). In addition to these two clinical features, the number of segments with peripheral lesions and GGO lesions, total CT score, total number of affected segments, air bronchogram, tree-in-bud sign, crazy-paving pattern, and subpleural curvilinear line were further used for multivariate logistic regression analysis. The number of segments with peripheral lesions, the number of segments with GGO, total number of affected segments, and total CT scores were categorized to 0 and 1 point according to the median (Table 4). Finally, the predictive model that included clinical and CT features for RT-PCR positivity was established (Fig. 3). AUC values of this model in the training and testing groups were 0.919 and 0.914, respectively ($p < 0.001$) (Fig. 4). After β was divided by 1.5, a predictive score for COVID-19 (PSC-19) was calculated based on the predictive model by the following formula: PSC-19 = 2 × history of exposure (0–1 point) − 1 × leukocyte count (0–2 points) + 1 × number of segments with peripheral lesions (0–1 point) + 2 × crazy-paving pattern (0–1 point). Thus, the total score ranges from −2 to 5 points, and all cut-off

values of the scores are presented in Table 5. An optimal cutoff point of 1 was chosen, with a sensitivity of 91.9% and a specificity of 66.1% in the training group, and a sensitivity of 88.5% and a specificity of 91.7% in the testing group. Examples of high and low PSC-19 for the diagnosis of COVID-19 and non-COVID-19 pneumonia are shown in Figs. 5 and 6, respectively.

Discussion

The main finding of the present study was that we managed to develop a risk prediction model for the presence of COVID-19 in patients presenting with signs and symptoms of pneumonia that was based on clinical, laboratory, and CT imaging findings in a training group of 118 patients, and comprised history of exposure to people infected with COVID-19, normal or decreased leukocyte count, a high number of lung segments with pathologic CT findings including peripheral dominance of lesions and presence of crazy-paving patterns as risk factors for COVID-19. The model was validated in a test group of 50 patients showing that distinction of COVID-19 was possible with high test quality parameters in an ROC analysis.

Table 3 Patients' radiological findings

| Radiological characteristics	COVID-19 ($n = 88$)	Non-COVID-19 ($n = 80$)	Overall ($n = 168$)	p value
Onset-CT interval (days)	5.5 (3.3, 7.8)	3.0 (1.3, 6.0)	4.0 (2.0, 7.0)	< 0.001
Lobes involved	4.0 (2.0, 5.0)	2.0 (1.0, 3.0)	3.0 (1.0, 4.0)	< 0.001
Segments involved	8.0 (3.3, 12.0)	3.0 (1.0, 5.0)	5.0 (2.0, 9.0)	< 0.001
Pulmonary infiltration (number of segments involved, at the segmental level)				
Density				
GGO	7.0 (3.0, 11.0)	2.0 (1.0, 4.0)	4.0 (1.0, 8.0)	< 0.001
Consolidation	5.0 (2.0, 10.0)	2.0 (1.0, 3.0)	3.0 (1.0, 6.8)	< 0.001
Location				
Periphery	8.0 (3.3, 12.0)	2.0 (1.0, 4.0)	4.0 (2.0, 8.0)	< 0.001
Center	0.0 (0.0, 2.0)	1.0 (0.0, 2.8)	1.0 (0.0, 2.0)	0.188
Form				
Patchy	5.0 (2.0, 11.0)	2.0 (1.0, 4.0)	4.0 (1.0, 8.0)	< 0.001
Oval	0.0 (0.0, 2.0)	0.0 (0.0, 1.0)	0.0 (0.0, 1.0)	0.130
CT score	14.0 (7.0, 24.5)	7.0 (2.0, 12.0)	9.0 (4.0, 17.0)	< 0.001
Other radiological patterns (at the patient level)				
Air bronchogram	54, 61.4%	32, 40.0%	86, 51.2%	0.006
Tree-in-bud sign	2, 2.3%	10, 12.5%	12, 7.1%	< 0.001
Crazy-paving pattern	59, 67%	12, 15.0%	71, 42.3%	< 0.001
Subpleural curvilinear line	19, 21.6%	7, 8.8%	26, 15.5%	0.022
Bronchiectasis	17, 19.3%	1, 1.3%	18, 10.7%	< 0.001
Air space	6, 6.8%	2, 2.5%	8, 4.8%	0.191
Lymphadenopathy	2, 2.3%	1, 1.3%	3, 1.8%	0.618
Pleural effusion	4, 4.5%	5, 6.3%	9, 5.4%	0.625

COVID-19 coronavirus disease 2019, *GGO*, ground glass opacity

Table 4 Categorized scores for clinical, laboratory, and radiological results

	Points		
	0	1	2
Clinical characteristics			
History of exposure	Without	With	–
Laboratory tests			
Leukocyte count	$< 3.5 \times 10^9$ per L	3.5–9.5×10^9 per L	$> 9.5 \times 10^9$ per L
Neutrophil count	$< 1.8 \times 10^9$ per L	1.8–6.3×10^9 per L	$> 6.3 \times 10^9$ per L
Platelet count	$< 125 \times 10^9$ per L	125–350×10^9 per L	$> 350 \times 10^9$ per L
CT findings			
Number of segments with peripheral lesions	≤ 4	> 4	–
Number of segments with GGO	≤ 4	> 4	–
Total number of affected segments	≤ 5	> 5	–
Total CT scores	≤ 8	> 8	–
Air bronchogram	Without	With	–
Tree-in-bud sign	Without	With	–
Crazy-paving pattern	Without	With	–
Subpleural curvilinear line	Without	With	–

GGO ground glass opacity

Fig. 2 ROC curve of the predictive model based on the clinical data. **a** AUC for the training group is 0.813 (95% CI, 0.735–0.891); **b** AUC for the testing group is 0.849 (95% CI, 0.737–0.961). Black points represent the cut-off values. ROC, receiver operating characteristic; AUC, area under curve; CI, confidence interval
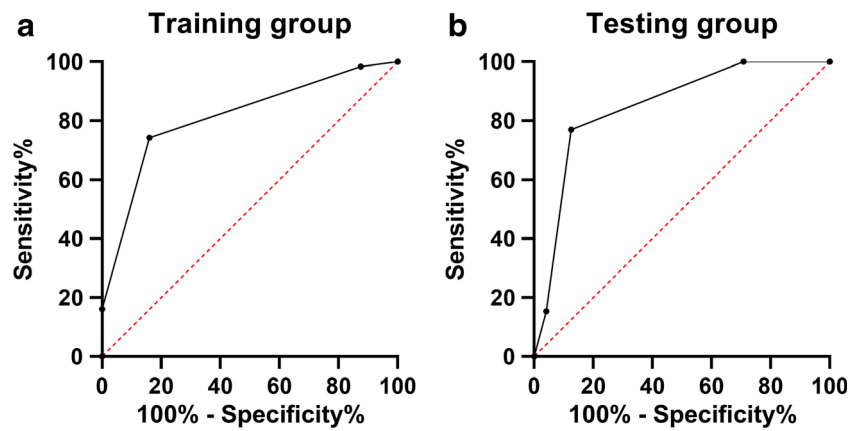
Since the outbreak of COVID-19 in Wuhan, China, history of exposure has been deemed as an important diagnostic criteria for COVID-19 [5]. However, the exact role of it in the diagnosis has still remained elusive. Our current research demonstrated that history of exposure was, but not the only strong predictor for the diagnosis of COVID-19. This result has great clinical values, especially for the current time when the number of cases is daily rising worldwide [12–14]. On one hand, with the increased number of cases and emergence of asymptomatic infectors, many suspected patients might have ambiguous history of exposure to COVID-19 [15]. On the other hand, in addition to direct human-to-human transmission, numerous patterns of transmission have been reported, including contact with contaminated fomites and inhalation of aerosols [16, 17]. It is noteworthy that in the present research, we included both COVID-19 patients without history of exposure and non-COVID-19 patients with history of exposure. Patients who were not confirmed or denied contact with infected cases were considered as without history of exposure. This is in accordance with the current trend that the infection source appears to be more obscure, as COVID-19 has become a pandemic worldwide. In addition, our study showed that compared with non-COVID-19 patients, COVID-19 patients had significantly lower leukocyte counts. That was reasonable because a proportion of non-COVID-19 patients were

clinically diagnosed as bacterial infection with high leukocyte count [18]. Thus, normal or abnormally low leukocyte count was found to be a significant clue for diagnosing COVID-19 [19].

To enhance the ability of clinical features to predict COVID-19-positive, CT features categorized to 0–1 point were further included to establish the predictive model in the present study. This is because CT can be rapidly and conveniently performed in the fever department, and plays a crucial role in the diagnosis of COVID-19 [20]. In a study of 1014 patients, Ai et al has reported that positive chest CT manifestations had high sensitivity for the diagnosis of COVID-19, and could also help indicate COVID-19-positive patients with initially negative but subsequently positive RT-PCR results [21]. Lin et al reported that in patients with laboratory-confirmed COVID-19 infection, abnormal CT findings can proceed clinical symptoms which could be useful to provide additional diagnostic information in asymptomatic population with history of exposure [22]. Furthermore, CT is sensitive enough to detect GGO lesions in the early stage of COVID-19 which can be easily overlooked in the chest radiography [23]. Thus, it is an indispensable component for the clinical diagnosis of COVID-19 [9]. Typical CT manifestations of COVID-19 have been described including GGO, mixed GGO, crazy-paving pattern, and multifocal lesions in a peripheral distribution [19, 24]. Efforts have also been

Fig. 3 Multivariate logistic regression analysis of patients' clinical and radiological findings. OR, odds ratio; CI, confidence interval

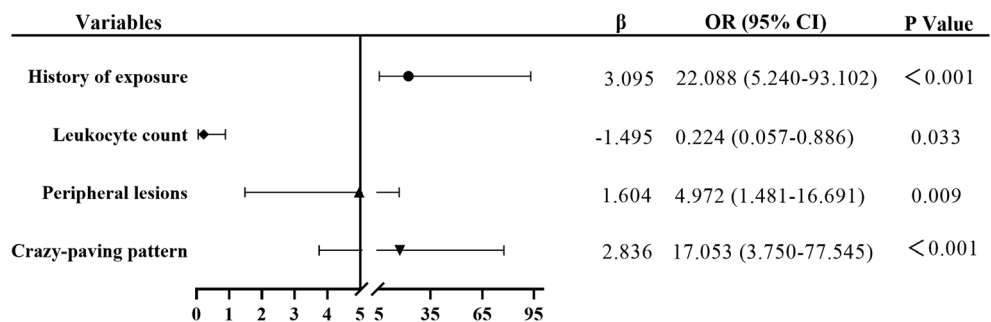| Variables	β	OR (95% CI)	P Value
History of exposure	3.095	22.088 (5.240–93.102)	<0.001
Leukocyte count	-1.495	0.224 (0.057–0.886)	0.033
Peripheral lesions	1.604	4.972 (1.481–16.691)	0.009
Crazy-paving pattern	2.836	17.053 (3.750–77.545)	<0.001

Fig. 4 ROC curve of the predictive model based on the clinical and radiological features. **a** AUC for the training group is 0.919 (95% CI, 0.871–0.967); **b** AUC for the testing group is 0.914 (95% CI, 0.824–1.000). Black points indicate the cut-off values. ROC, receiver operating characteristic; AUC, area under curve; CI, confidence interval
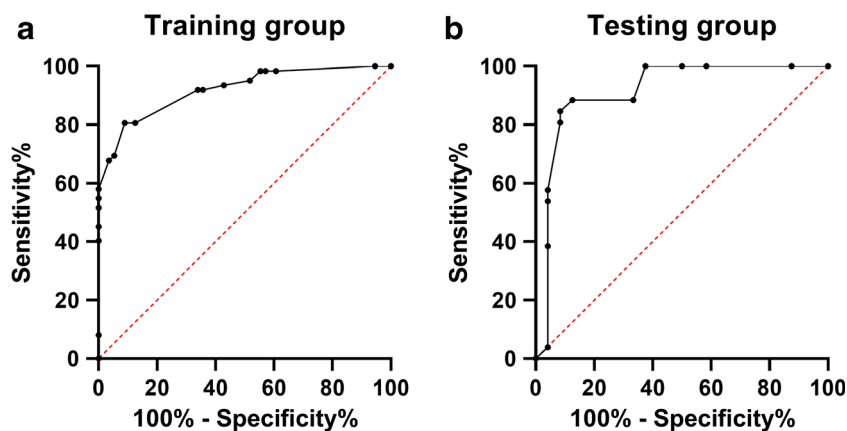
made to distinguish COVID-19 from other types of pneumonia by chest CT. Our preliminary study on 33 patients demonstrated that multifocal, peripheral, and GGO lesions predominately located in the lower lung field were likely to indicate COVID-19 [25]. An analysis of SARS revealed that nodule, cavitation, lymphadenopathy, and pleural effusion were rare findings which could assist differentiation of coronavirus infection from other types of viral pneumonia [26]. Recently, Bai et al reported that compared with other types of viral pneumonia, COVID-19 tended to have more peripheral and GGO lesions with reticular opacity and vascular thickening [27]. These features may make the diagnosis from radiologists more specific. Consistent with previous studies, the results of the

present study indicated that multiple segments with GGO and patchy lesions in peripheral distribution were significantly associated with COVID-19. The presence of other CT manifestations including air bronchogram, crazy-paving pattern, and subpleural curvilinear line, and the lack of the tree-in-bud signs for advantageous for diagnosis and differentiation as well. These manifestations were evidenced by the pathological findings observed in COVID-19. GGO and mixed GGO changes were reflected by alveolar edema, proteinaceous exudates, and vascular congestion, while crazy-paving pattern was associated with interstitial infiltration of inflammatory mononuclear cells dominated by lymphocyte [28, 29].

However, these clinical and radiological characteristics could not by quantitatively assessed, and a simple scoring system might be suitable for the management in the fever department. Our results showed that the predictive model established based on both clinical and radiological features had higher diagnostic efficiency than the model that developed on the basis of clinical data alone. This model also reflected the two most critical signs for the diagnosis: crazy-paving pattern and increased number of involved lung segments with peripheral predominance. Although GGO and the number of affected segments strongly indicated COVID-19, they were not included in the scoring system due to their high correlation with peripheral lesions. Based on the established predictive model, we proposed a scoring system called PSC-19 and suggested its optimal cutoff point showing the best diagnostic accuracy. PSC-19 employed full advantages of signs and features provided by CT and the corresponding clinical parameters, making it useful for physicians to apply in the fever department. Furthermore, due to the highly contagious nature of COVID-19, PSC-19 might be a potentially helpful tool for the fast detection, isolation, and management of suspected patients to prevent the spread of COVID-19.

This study has several limitations. First, the sample size was relatively small, and a study with a larger sample size should be therefore carried out. To enroll more

Table 5 Cut-off values of PSC-19 for the prediction of COVID-19-positive

Score	Sensitivity	Specificity
Training group		
−2	100%	0%
−1	100%	5.4%
0	98.4%	44.6%
1	91.9%	66.1%
2	69.4%	94.6%
3	51.6%	100%
4	8.1%	100%
5	0%	100%
Testing group		
−2	100%	12.5%
−1	100%	50%
0	100%	83.3%
1	88.5%	91.7%
2	61.5%	95.8%
3	38.5%	95.8%
4	3.8%	95.8%
5	0%	100%

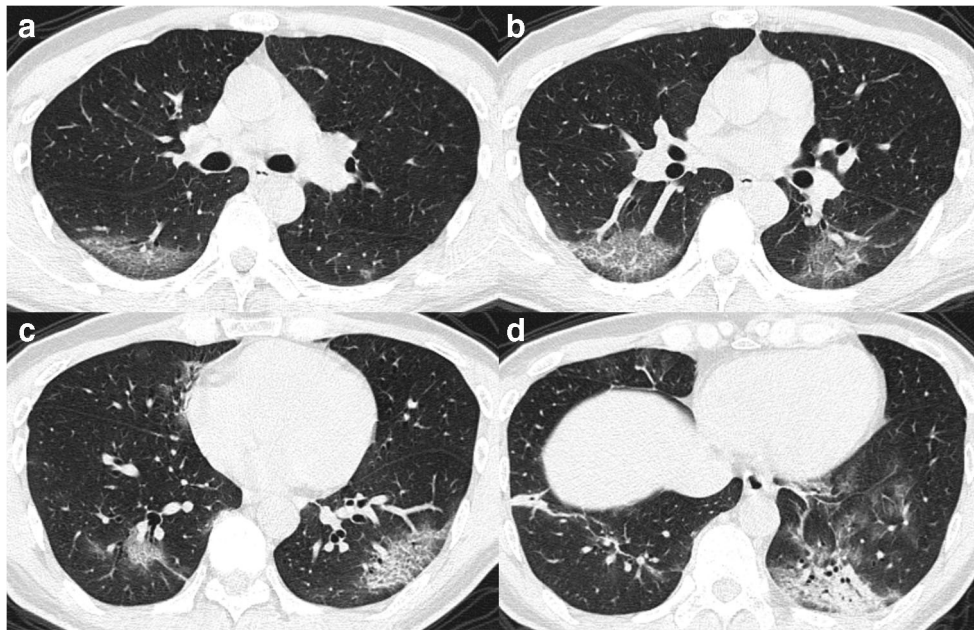*COVID-19* coronavirus disease 2019, *PSC-19* predictive score for COVID-19

Fig. 5 A 47-year-old male with the symptom of fever. He had a history of exposure to COVID-19 via contacting with individuals who came from Hubei Province. **a**–**d** Multiple peripheral lesions with GGO and consolidated attenuation were demonstrated, and crazy-paving pattern could be observed as well. PSC-19 for this patient was equal to 4, with 2 points for history of exposure, − 1 point for normal leukocyte count (5.4 × 10^9/L), 1 point for peripheral lesions (12 segments affected), and 2 points for crazy-paving pattern. The total score of 4 strongly indicated positive result of RT-PCR test for COVID-19. GGO, ground glass opacity; PSC-19, predictive score for COVID-19; RT-PCR, reverse transcription–polymerase chain reaction.

COVID-19 patients without history of exposure, Chinese patients living outside Hubei Province should be included. Second, the patients without chest CT were excluded which would result in potential selection bias. However, the purpose of our study was to take advantage of CT features to increase the diagnostic efficiency for COVID-19. Third, the etiology of some COVID-19-negative cases remained unknown. Due to the risk of

Fig. 6 A 34-year-old female with the symptoms of cough and fever. She had no history of exposure to COVID-19. **a**–**d** Centrally distributed and multifocal GGO lesions with patchy pattern were demonstrated. No peripheral lesions and crazy-paving pattern could be observed. PSC-19 for this patient was equal to − 2, with 0 point for history of exposure, − 2 points for abnormally high leukocyte count (10.68 × 10^9/L), 0 point for peripheral lesions, and 0 point for crazy-paving pattern. The total score of − 2 indicated negative result of RT-PCT test for COVID-19. GGO, ground glass opacity; PSC-19, predictive score for COVID-19; RT-PCR, reverse transcription–polymerase chain reaction
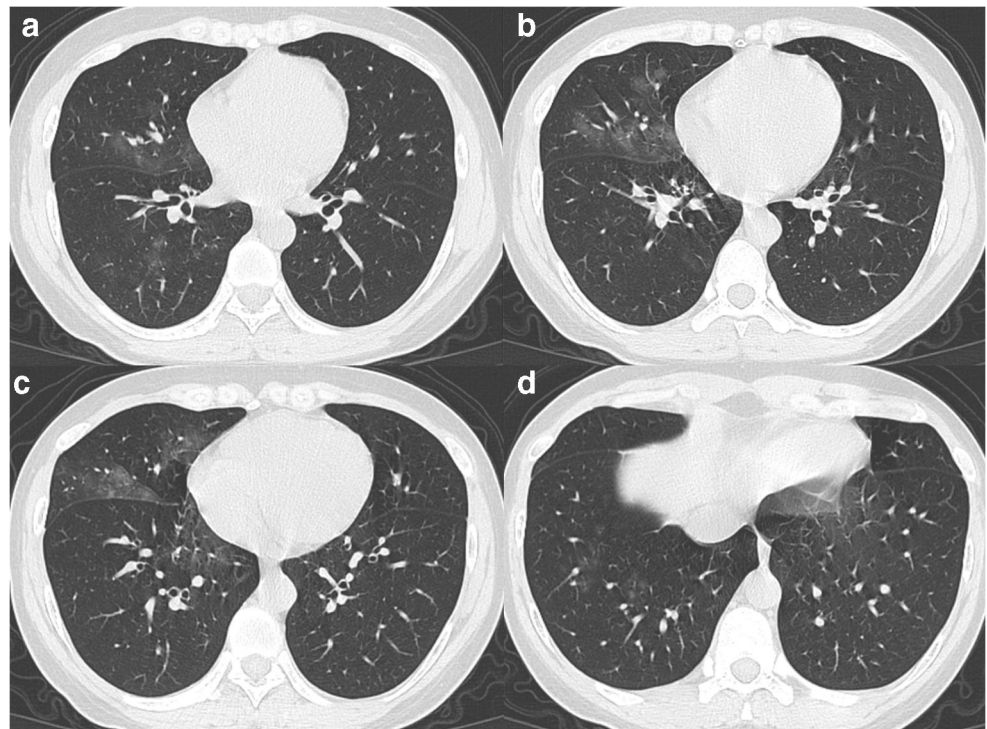
cross-infection in the hospital, a number of non-severe patients were discharged immediately after exclusion of COVID-19, and the complete pathogen examinations were not therefore undertaken. Finally, coagulation, biochemical, and other parameters associated with infection may be useful for the diagnosis of COVID-19, which should be included in the future study. However, in clinical practice, physicians are likely to have very limited laboratory data, and have to make a correct diagnosis shortly. Thus, our study might be helpful in the practice.

In conclusion, our study established a scoring system, namely PSC-19, which could be helpful for the prediction of COVID-19 in the fever department, assisting physicians and radiologists to reliably identify COVID-19-positive cases until receiving the results of RT-PCR tests.

Compliance with ethical standards

Guarantor The scientific guarantor of this publication is Wenjie Yang.

Conflict of interest The authors of this manuscript declare no relationships with any companies whose products or services may be related to the subject matter of the article.

Statistics and biometry Dr. Qiyuan Bao kindly provided statistical advice for this manuscript.

Informed consent Written informed consent was waived by the Institutional Review Board.

Ethical approval Institutional Review Board approval was obtained.

Methodology
• retrospective
• diagnostic or prognostic study/observational
• multicenter study

References

1. Zhu N, Zhang D, Wang W et al (2020) A novel coronavirus from patients with pneumonia in China, 2019. N Engl J Med 382:727–733
2. Huang C, Wang Y, Li X et al (2020) Clinical features of patients infected with 2019 novel coronavirus in Wuhan, China. Lancet 395:497–506
3. Chan JF, Yuan S, Kok KH et al (2020) A familial cluster of pneumonia associated with the 2019 novel coronavirus indicating person-to-person transmission: a study of a family cluster. Lancet 395:514–523
4. Chen N, Zhou M, Dong X et al (2020) Epidemiological and clinical characteristics of 99 cases of 2019 novel coronavirus pneumonia in Wuhan, China: a descriptive study. Lancet 395:507–513
5. Li Q, Guan X, Wu P et al (2020) Early transmission dynamics in Wuhan, China, of novel coronavirus–infected pneumonia. N Engl J Med 382:1199–1207
6. Fang Y, Zhang H, Xie J et al (2020) Sensitivity of chest CT for COVID-19: comparison to RT-PCR. Radiology. https://doi.org/10.1148/radiol.2020200432
7. Xie X, Zhong Z, Zhao W, Zheng C, Wang F, Liu J (2020) Chest CT for typical 2019-nCoV pneumonia: relationship to negative RT-PCR testing. Radiology. https://doi.org/10.1148/radiol.2020200343
8. Huang P, Liu T, Huang L et al (2020) Use of chest CT in combination with negative RT-PCR assay for the 2019 novel coronavirus but high clinical suspicion. Radiology 295:22–23
9. Committee GOoNH (2020) Office of State Administration of Traditional Chinese Medicine. Notice on the issuance of a program for the diagnosis and treatment of novel coronavirus (2019-nCoV) infected pneumonia (trial sixth edition)
10. Mandell LA, Wunderink RG, Anzueto A et al (2007) Infectious Diseases Society of America/American Thoracic Society consensus guidelines on the management of community-acquired pneumonia in adults. Clin Infect Dis 44:S27e72
11. Hansell DM, Bankier AA, MacMahon H, McLoud TC, Müller NL, Remy J (2008) Fleischner Society: glossary of terms for thoracic imaging. Radiology 246:697–722
12. Lim J, Jeon S, Shin HY et al (2020) Case of the index patient who caused tertiary transmission of COVID-19 infection in Korea: the application of lopinavir/ritonavir for the treatment of COVID-19 infected pneumonia monitored by quantitative RT-PCR. J Korean Med Sci 35:e79
13. COVID-19 National Incident Room Surveillance Team (2020) COVID-19, Australia: epidemiology report 2: reporting week ending 19:00 AEDT 8 February 2020. Commun Dis Intell (2018) https://doi.org/10.33321/cdi.32020.33344.33314
14. Eurosurveillance Editorial Team (2020) Latest updates on COVID-19 from the European Centre for Disease Prevention and Control. Euro Surveill. https://doi.org/10.2807/1560-7917
15. Hoehl S, Rabenau H, Berger A et al (2020) Evidence of SARS-CoV-2 infection in returning travelers from Wuhan, China. N Engl J Med 382:1278–1280
16. Guan W-J, Ni Z-Y, Hu Y et al (2020) Clinical characteristics of coronavirus disease 2019 in China. N Engl J Med 382:1708–1720
17. Rothe C, Schunk M, Sothmann P et al (2020) Transmission of 2019-nCoV infection from an asymptomatic contact in Germany. N Engl J Med 382:970–971
18. Huang Y, Liu A, Liang L et al (2018) Diagnostic value of blood parameters for community-acquired pneumonia. Int Immunopharmacol 64:10–15
19. Song F, Shi N, Shan F et al (2020) Emerging coronavirus 2019-nCoV pneumonia. Radiology 295:210–217
20. Pan Y, Guan H, Zhou S et al (2020) Initial CT findings and temporal changes in patients with the novel coronavirus pneumonia (2019-nCoV): a study of 63 patients in Wuhan, China. Eur Radiol. https://doi.org/10.1007/s00330-020-06731-x
21. Ai T, Yang Z, Hou H et al (2020) Correlation of chest CT and RT-PCR testing in coronavirus disease 2019 (COVID-19) in China: a report of 1014 cases. Radiology. https://doi.org/10.1148/radiol.2020200642
22. Lin C, Ding Y, Xie B et al (2020) Asymptomatic novel coronavirus pneumonia patient outside Wuhan: the value of CT images in the course of the disease. Clin Imaging 63:7–9
23. Zu ZY, Jiang MD, Xu PP et al (2020) Coronavirus disease 2019 (COVID-19): a perspective from China. Radiology. https://doi.org/10.1148/radiol.2020200490

24. Chung M, Bernheim A, Mei X et al (2020) CT imaging features of 2019 novel coronavirus (2019-nCoV). Radiology 295:202–207

25. Cheng Z, Lu Y, Cao Q et al (2020) Clinical features and chest CT manifestations of coronavirus disease 2019 (COVID-19) in a single-center study in Shanghai, China. AJR Am J Roentgenol. https://doi.org/10.2214/AJR.20.22959

26. Koo HJ, Lim S, Choe J, Choi SH, Sung H, Do KH (2018) Radiographic and CT features of viral pneumonia. Radiographics 38:719–739

27. Bai HX, Hsieh B, Xiong Z et al (2020) Performance of radiologists in differentiating COVID-19 from viral pneumonia on chest CT. Radiology. https://doi.org/10.1148/radiol.2020200823

28. Tian S, Hu W, Niu L, Liu H, Xu H, Xiao SY (2020) Pulmonary pathology of early-phase 2019 novel coronavirus (COVID-19) pneumonia in two patients with lung cancer. J Thorac Oncol 15(5):700 –704. https://doi.org/10.20944/preprints202002.0220.v1

29. Xu Z, Shi L, Wang Y et al (2020) Pathological findings of COVID-19 associated with acute respiratory distress syndrome. Lancet Respir Med 8:420–422

Publisher's note Springer Nature remains neutral with regard to jurisdictional claims in published maps and institutional affiliations.